Simulations of Deep-Level Defects in Semiconductors

António Resende
School of Physics, University of Exeter, Exeter EX4 4QL, UK

April 19, 1999

Abstract

Experimental and theoretical investigations into divacancies in Si are reviewed. The results of EPR, DLTS and theoretical modelling are described in detail.

ENDEASD

European Network on Defect Engineering of Advanced Semiconductor Devices

UNIVERSITY of EXETER

Talk overview

The lattice divacancy in silicon

- ☐ How is this native defect created?
- ☐ What techniques are used to detect and study it?
- ☐ What are its structural and electrical properties?
- ☐ Recent advances in theory

The lattice divacancy in silicon

The lattice divacancy (V_2) is one of the most important native defects in irradiated and/or implanted silicon...

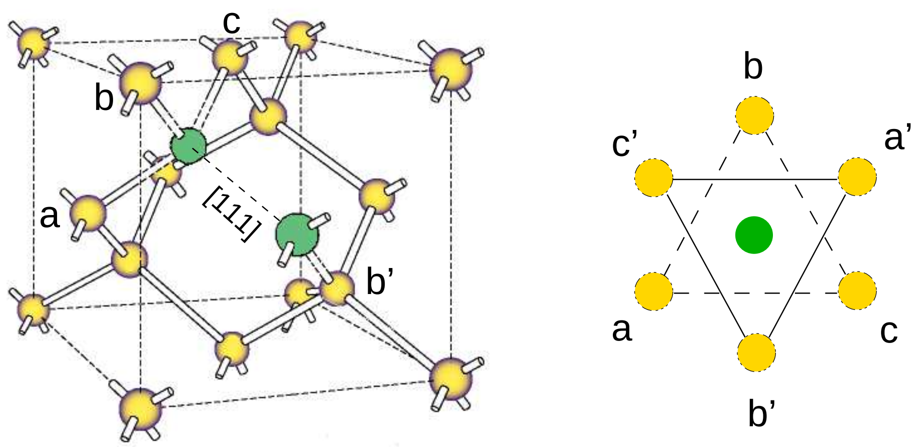

It can be defined as two nearby monovacancies sharing a unpaired 'dangling-bond'.

- V_2 defects are unavoidably created during any of the following processing steps:
  – ion-implantation, electron-beam lithography or plasma etching

- Intentionally, by irradiation or implantation at room-temperature of: electrons (e^-), protons (H^+), α-particles (He^{2+}), heavier ions, neutrons (n) or γ-rays

- Appears in both Czochralski (O-rich) and float-zone Si, irrespectively of the dopant type

Experimental tools

V_2 is known to:

- □ be immobile and stable at room temperature
- □ anneal out $\sim$ 200–300 °C

Its properties have been studied over the last 3 decades by:

- □ Electron-paramagnetic resonance (EPR)
- □ Electron-nuclear double resonance (ENDOR)
- □ Photoluminescence (PL)
- □ Infra-red (IR) absorption
- □ Photoconductivity measurements
- □ Deep-level transient spectroscopy (DLTS)
- □ Positron-annihilation spectroscopy

The "defect-molecule" model

One-electron model for the single vacancy in Si (LCAO-MO):

$$\Psi = \sum_i^4 \eta_i \overbrace{(a_i\,(\psi_s)_i + b_i\,(\psi_p)_i)}^{\psi_i} \quad \text{with} \quad a_i^2 + b_i^2 = 1$$

Eigenvalue problem: $\widehat{\mathcal{H}}\,\Psi = E\,\Psi$

$$\det|\widehat{\mathcal{H}} - E\,\widehat{\mathcal{S}}| = 0 \quad \text{with} \quad \begin{array}{c} <\psi_i\,|\,\widehat{\mathcal{H}}\,|\,\psi_i> = 0 \\ <\psi_i\,|\,\widehat{\mathcal{H}}\,|\,\psi_j> = \beta \\ S_{ij} = <\psi_i\,|\,\psi_j> \equiv \delta_{ij} \end{array}$$

– Diagonalization of

$$\begin{bmatrix} -E & \beta & \beta & \beta \\ \beta & -E & \beta & \beta \\ \beta & \beta & -E & \beta \\ \beta & \beta & \beta & -E \end{bmatrix} \Rightarrow \begin{array}{l} E(A_1) = 3\beta \\ E(T_2) = -\beta \end{array}$$

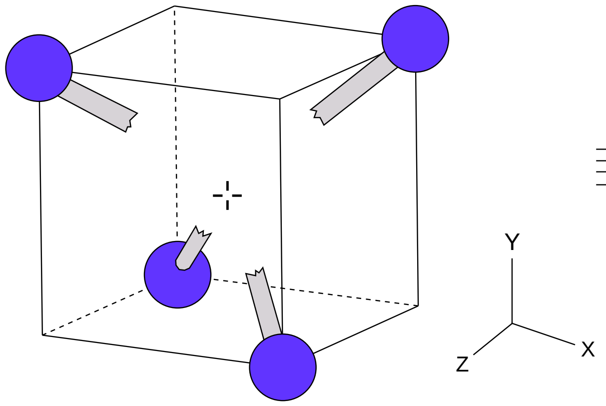

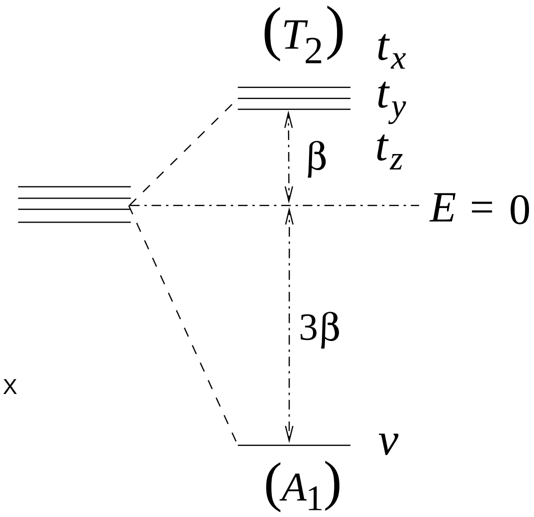

$$v = \frac{1}{2}\{\psi_1 + \psi_2 + \psi_3 + \psi_4\};\, t_x = \frac{1}{2}\{\psi_1 + \psi_2 - \psi_3 - \psi_4\}$$

LCAO-MO model of V_2 from EPR

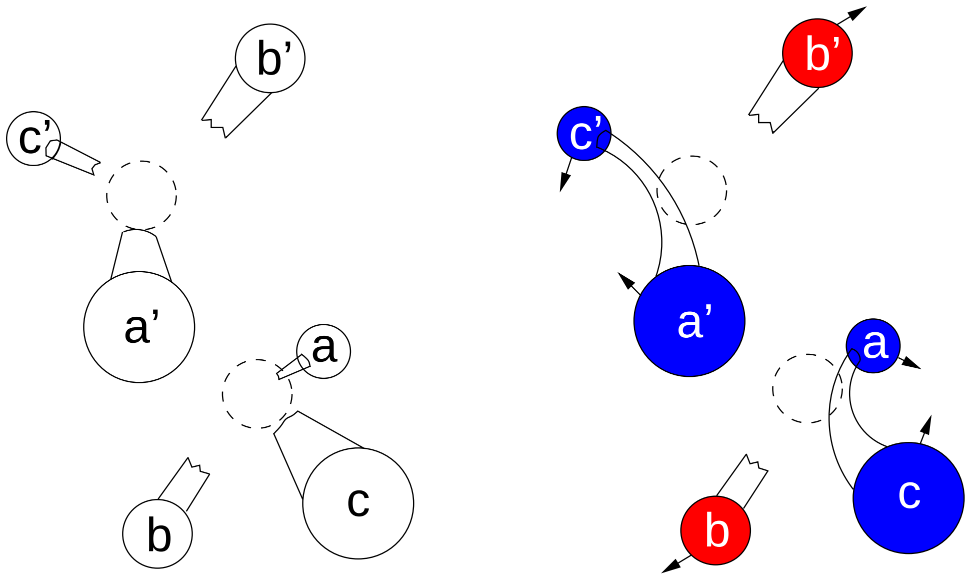

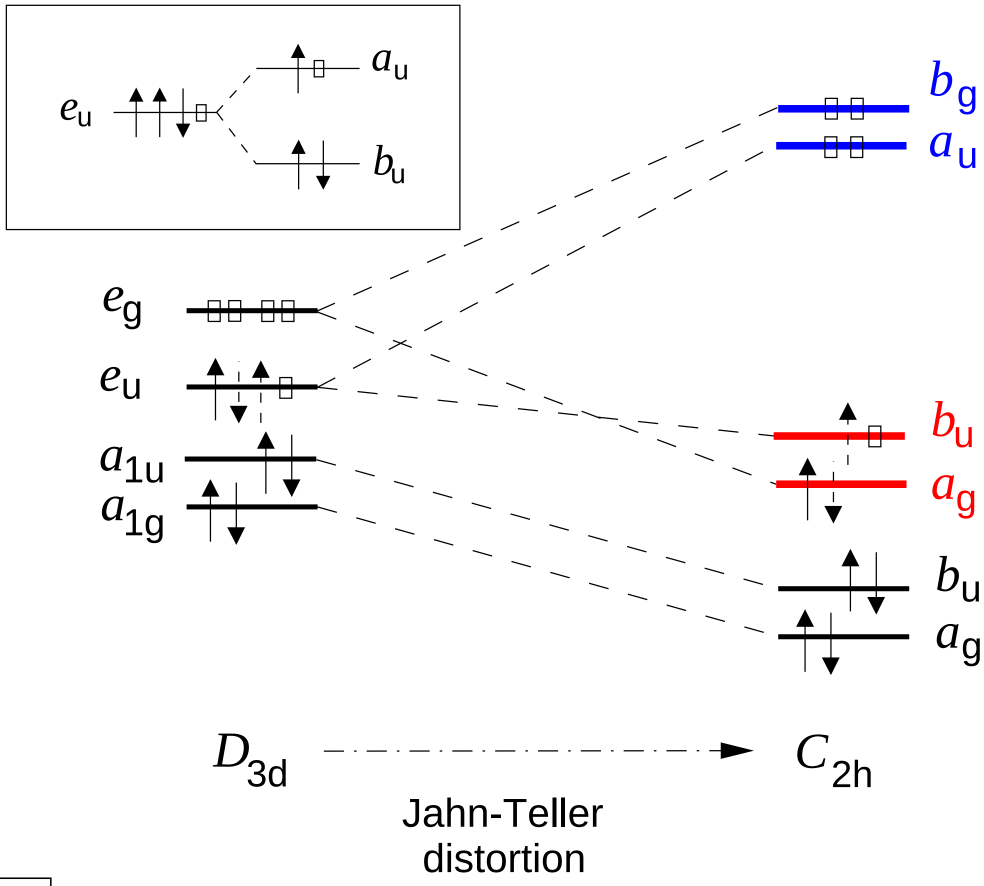

Information derived from EPR

The divacancy is a perfect example of the power of EPR. From the experiments of Watkins and Corbett...

It is known that. . .	From. . .
G6 (V_2^+) & G7 (V_2^-): $S = \frac{1}{2}$	$\overleftrightarrow{g}$, fine structure
2 equivalent Si nuclei	^{29}Si hf satellites vs. $\vec{B}$ (4.7%, $I = \frac{1}{2}$) $\overleftrightarrow{A}_{\mathrm{b}} = \overleftrightarrow{A}_{\mathrm{b}'}$
C_{2h} symmetry at $T < 40$ K	$\overleftrightarrow{A}_i$ & $\overleftrightarrow{g}$ shifts with $\vec{B}$ Low-T stress studies
60% of wf localised on b & b′ $\sim$ 70% on the 6 atoms	hf interaction analysis via a_i^2, b_i^2 and η_i^2
$E_{\mathrm{Jahn-Teller}}(V_2^+) \sim 1.3$ eV $E_{\mathrm{Jahn-Teller}}(V_2^-) \sim 2.4$ eV 'bond switching' $\Delta E \sim 0.06$ eV	Low-T stress studies
Motional narrowing: $C_{2h} \rightarrow D_{3d}$ T-activated reorientation	Linewidth vs. T ($40 < T < 110$ K)
ΔE for diffusion: $\sim$ 1.3 eV (V_2^0)	High-T stress studies

Structural manifestation of the Jahn-Teller effect

A "Mexican Hat"...

The potential surface V for a doubly degenerate state and a contour map of $V(Q_2, Q_3)$ including anharmonic terms

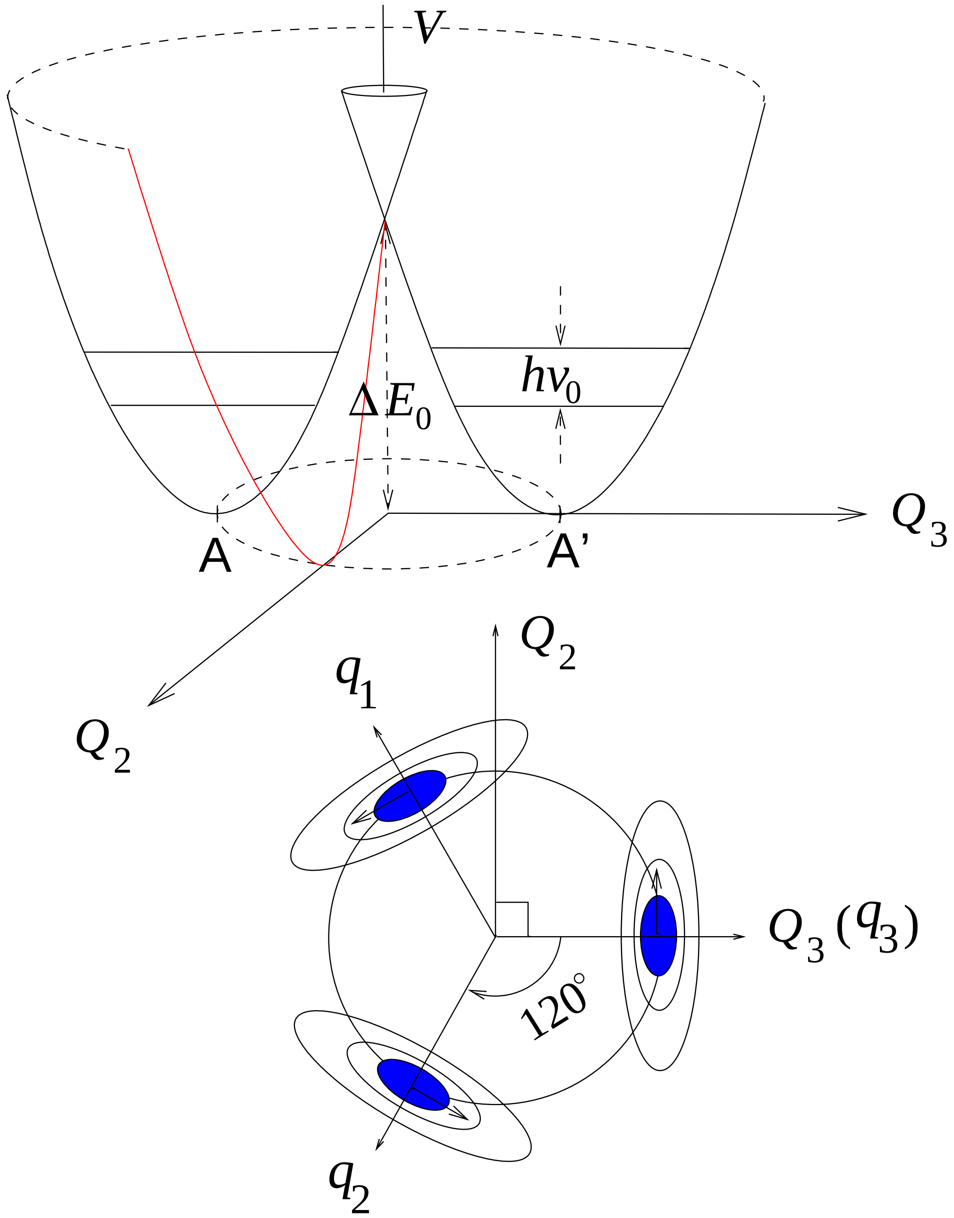

Electrical activity

EPR and DLTS studies have provided two slightly different pictures for the level structure of the lattice divacancy in Si:[1]

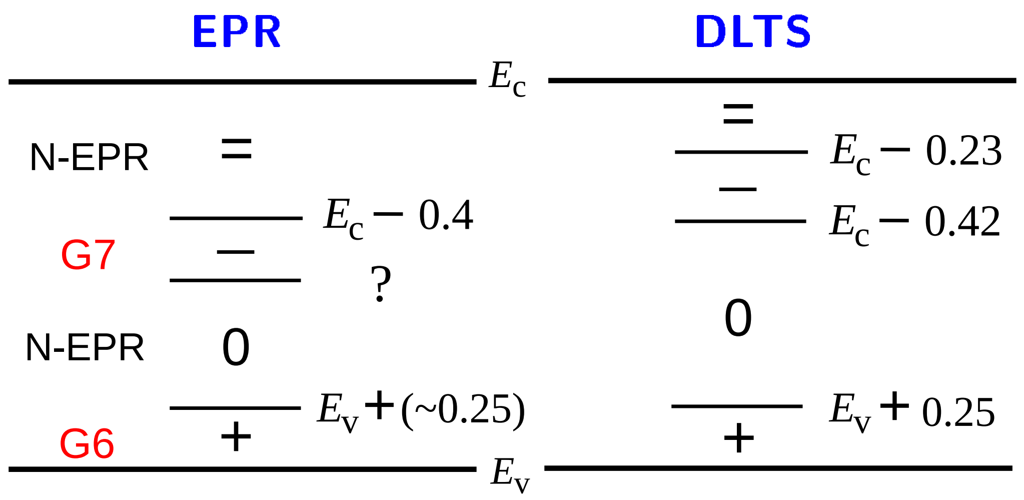

It is importante to note that:

- For $T \leqslant 40$ K (EPR), the unpaired electron is trapped in one of its 3 equivalent JT distortion directions
  $\Rightarrow$ C_{2h} symmetry.

- In DLTS, $80 < T < 250$ K, the electronic jump rate between equivalent Jahn-Teller directions and the rate for electron emission relate as follows:

$$\frac{1}{\tau}\,(\text{jump EPR}) \gg \frac{1}{\tau}\,(\text{emission DLTS})$$

$\Rightarrow$ "Motionally average" state (D_{3d})

[1] EPR: G. D. Watkins and J. W. Corbett, Phys. Rev. **138**, A543 (1965); DLTS: A. O. Evwaraye and E. Sun, J. Appl. Phys. **47**, 3776 (1976).

The Poole-Frenkel effect

Electron emission enhancement under an electrical field

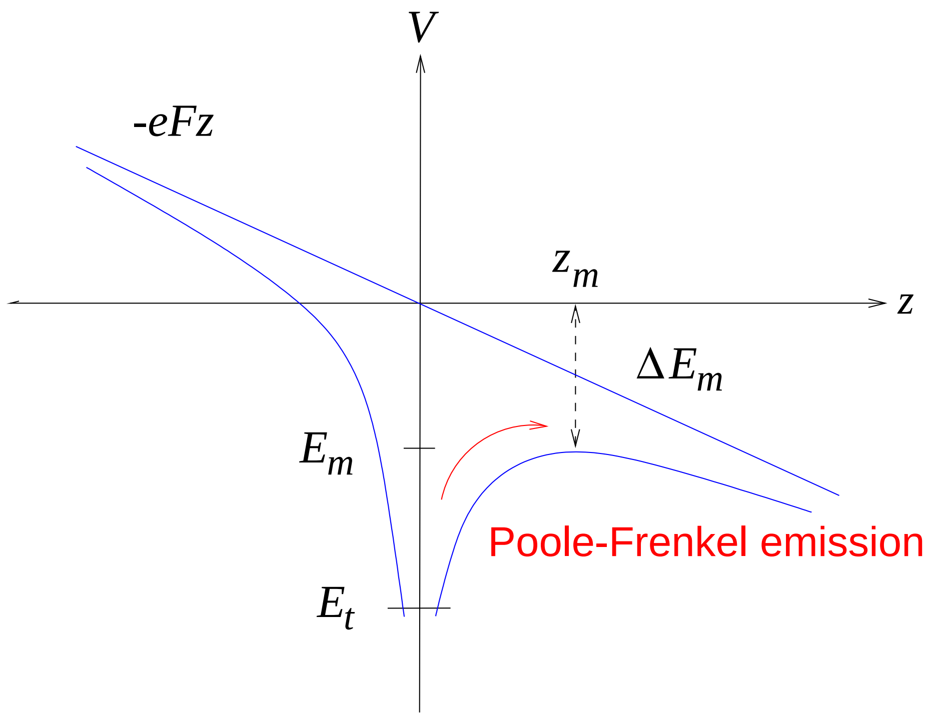

$$g_e \propto \exp\left\{-\frac{E_t - \Delta E_m}{k_B\,T}\right\}$$

$$V_{\text{defect}} = -\frac{e^2}{\epsilon_c\, r} \Rightarrow \Delta E_m = 2e\sqrt{\frac{eF}{\epsilon_c}}$$

▷ The study of the ΔE_m vs. F ($\Delta E_m \propto F^{1/2}$) is a possible way of determining the donor or acceptor character of the centre!

DLTS results

There is still some debate on the assignments of the charge states $2-$, $-$ and 0, of V$_2$ to the peaks observed by DLTS...

☐ The reported electron-capture cross-sections (σ_n) *have not* confirmed a double acceptor character for the $E_c - 0.23$ eV DLTS trap (H$^+$-irradiated samples), *e.g.*

$$\sigma_n(=/-) = 2.6 \times 10^{-15}\ \text{cm}^2 \quad : E_c - 0.23\ \text{eV}$$
$$\sigma_n(-/0) = 1.7 \times 10^{-15}\ \text{cm}^2 \quad : E_c - 0.43\ \text{eV}$$

▷ σ_n for a $(=/-)$ level is typically $\sim 10^{-18}$–10^{-21} cm^2; unexpectedly, no Poole-Frenkel was ever reported for V$_2(=/-)$!

☐ From depth profiling studies, it was observed that:

– MeV-e irradiation

$$\frac{[\text{V}_2(-/0)]}{[\text{V}_2(=/-)]} = 1$$

– H$^+$, He^{2+} or heavier ions

$$\frac{[\text{V}_2(-/0)]}{[\text{V}_2(=/-)]} \gg 1$$

▷ It has been argued[2] that the formation of V$_2^{2-}$ (D_{3d}) is improbable in highly damaged regions of the sample – the high-T bond-switching does not occur, with the distortion acting to relief the strain around the defect.

[2] Svensson *et al.*, Phys. Rev. B **43**, 2292 (1991).

Modelling

The common denominator to all the recent theoretical studies on V_2 is...

Density Functional Theory (DFT):

Electron density is a quantity of fundamental importance

The Kohn-Sham scheme allows a description of the many body-problem as a set of self-consistent one-electron equations:

$$\left\{ -\frac{1}{2}\nabla^2 + V_{\text{eff}}(\vec{r}) \right\} \psi_j(\vec{r}) = \varepsilon_j \, \psi_j(\vec{r})$$

$$V_{\text{eff}} = v_{i-e} + v_{\text{Hartree}} + v_{xc} \quad \text{and} \quad n(\vec{r}) = \sum_j |\psi_j(\vec{r})|^2$$

- ☐ v_{xc} (exchange-correlation term) assumed to be something simple – Local density approximation (LDA): electron-gas of slow-varying density
- ☐ Core electrons are removed by using norm-conserving pseudopotentials: only valence electrons come into play
- ☐ Write ψ_is as sum of plane-wave or Cartesian Gaussian orbitals
- ☐ The crystalline environment of the defects is simulated by: periodic super-cells or H-terminated atomic clusters

Simulating bulk silicon

Clusters vs. Supercells

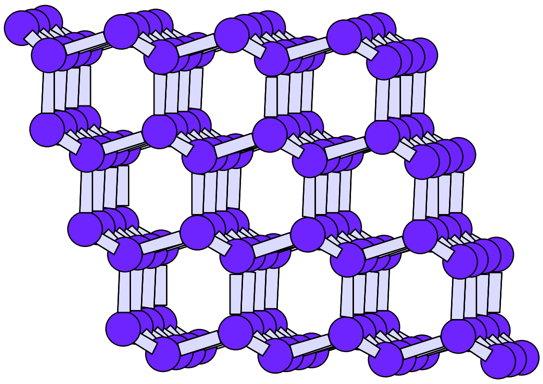

128-atom *fcc* supercell

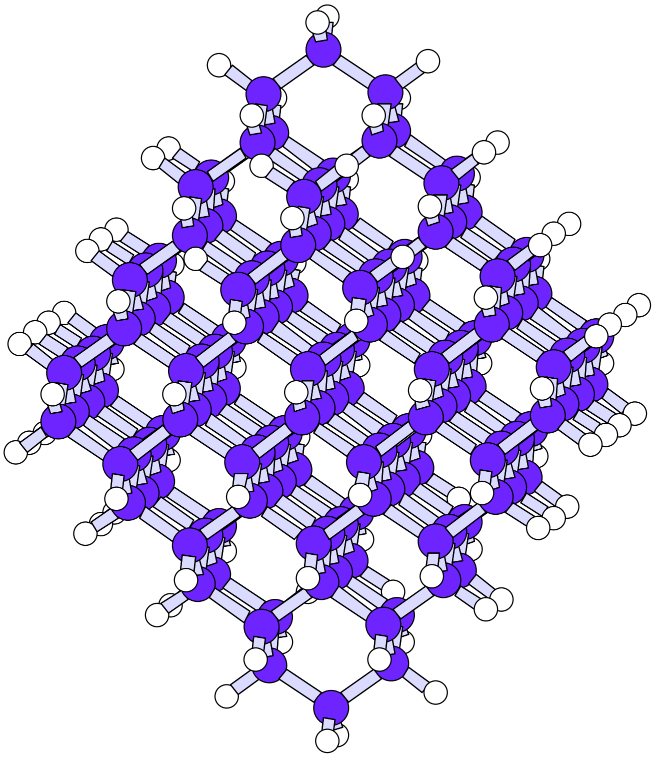

bond-centred $Si_{148}H_{98}$ cluster

▷ The spatial extent of the divacancy wavefunction is of particular importance. The system size has to be large enough to avoid:

- ☐ defect-defect interactions (supercells)
- ☐ defect-surface interactions (clusters)

Calculation of electrical levels

In order to understand the electrical properties of V_2, the prediction of its electrical-level structure is of great importance...

▷ A donor level with respect to E_v is the difference between the ionization energy of bulk Si and that of the defect, i.e.

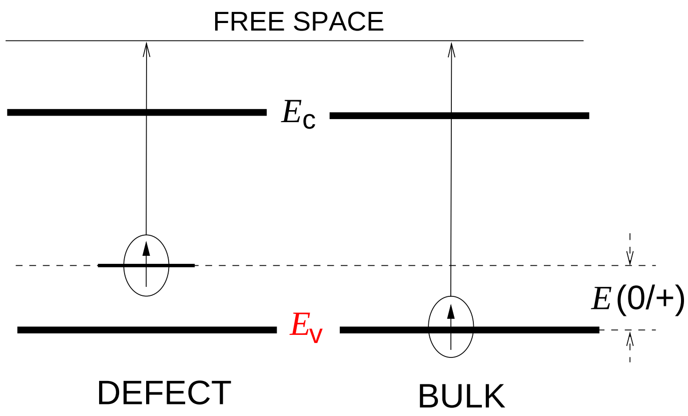

$$E(0/+)_d = I_b - I_d$$

▷ To overcome difficulties on calculating the ionization energy of bulk Si, we compare the ionization energies of the defect and a standard defect with well-known electrical levels

$$E(0/+)_d = \overbrace{(I_s + (E(0/+)_s)}^{I_b} - I_d$$

$E(0/+)_s \equiv$ observed donor level of the standard defect.

▷ The affinity and ionisation potentials are calculated by applying Slater's "transition state" scheme.

Previous theoretical studies: A. Saito & Oshiyama

Recently, Saito and Oshiyama[3] have proposed a new model for the structure of V_2, and in particular V_2^-...

▷ For V_2^-, the sense of the Jahn-Teller (JT) distortion is the inverse of that proposed by Watkins & Corbett (pairing model)

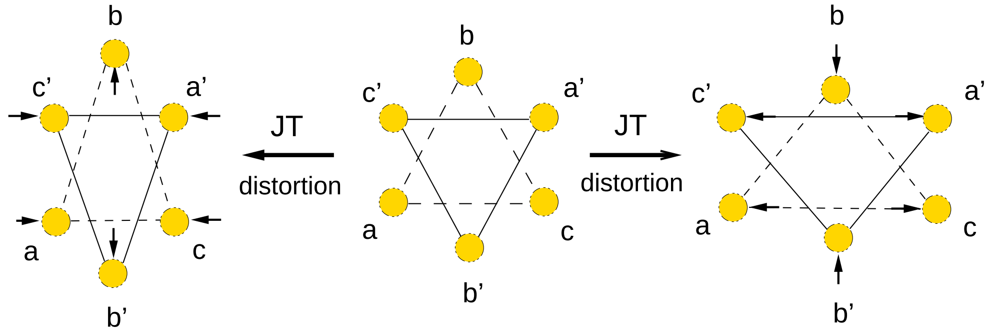

C_{2h}	D_{3d}	C_{2h}
Pairing model (P)	Breathing model (B)	"resonant-bond" model (R)
$l_{ac} < l_{ab} = l_{bc}$	$l_{ab} = l_{ac} = l_{ac}$	$l_{ab} = l_{ac} > l_{ac}$

According to this model, the one-electron configurations of V_2 in its paramagnetic charge states are:

$$V_2^+ : (a_u)^1 (b_u)^0 \quad \text{and} \quad V_2^- : (a_u)^2 (b_u)^1$$

▷ Note that the a_u level has no amplitude on the mirror plane!

[3] 64-atom cubic supercells – M. Saito and A. Oshiyama, Phys. Rev. Lett. **73**, 866 (1994).

Previous theoretical studies: B. Pesola, von Boehm, Pöykkö and Nieminen

Pesola *et al.*[4] have suggested that the distortion exhibited by V_2^- is mixture between a "rebonding-by-pairs" distortion and a "resonant-bond" one.

▷ This group was able to predict the electrical structure of V_2 by first principles...

Table I. Calculated and electrical levels of V_2 for different supercell sizes.

	supercell		Obs.	
Level	216	128	EPR	DLTS
$(=/-)$	$E_c - 0.73$	$E_c - 0.69$	$E_c - 0.40$	$E_c - 0.23$
$(-/0)$	$E_c - 0.78$	$E_c - 0.84$	$E_c - 0.61^*$	$E_c - 0.42$
$(0/+)$	$E_v + 0.04$	$E_v + 0.03$	$E_v + 0.25$	$E_v + 0.25$

* Positron annihilation spectroscopic studies

[4] M. Pesola, J. von Boehm, S. Pöykkö and R. M. Nieminen, Phys. Rev. B, **58**, 1106 (1998).

Results: A. Energetics

▷ The structure proposed by Saito and Oshiyama was found to be unstable, relaxing spontaneously to a metastable "rebonding-by-pairs"–like structure: weak pairing

Table II. Differences in total energies (eV) for the several competing configurations of V_2 in four difference charge states.

Energy diff.	V_2^{2-}	V_2^{-}	V_2^{+}
strong pairing	0	0	0
D_{3d}	$+0.5$	$+0.4$	$+0.3$
weak pairing	$+0.4$	$+0.3$	$+0.6$

Results: B.
Structural parameters

Table III & IV. Calculated distances (Å) for Si atoms surrounding a V_2 defect, for two different charge states.

	l_{ab}	l_{bc}	l_{ac}	Type	Symm.	Ref.
	3.75	3.75	3.61	**P**	C_{2h}	[1]
V_2^+	3.55	3.56	3.17	**P**	C_{2h}	[2]
	3.78	3.78	2.92	**P**	C_{2h}	

	l_{ab}	l_{bc}	l_{ac}	Type	Symm.	Ref.
	3.60	3.60	3.69	**R**	C_{2h}	[1]
V_2^-	3.55	3.52	3.45	**M**(P)	S_2	[2]
	3.71	3.71	2.76	**P**	C_{2h}	

[1] M. Saito and A. Oshiyama, PRL **73**, 866 (1994).
(64-atom supercells; 8-Ry cut-off)

[2] M. Pesola, J. von Boehm, S. Pöykkö and R. M. Nieminen, PRB, **58**, 1106 (1998).
(64-supercell; 15-Ry cut-off)

Results: C.
Spin density localisation

One-electron picture for V_2^-

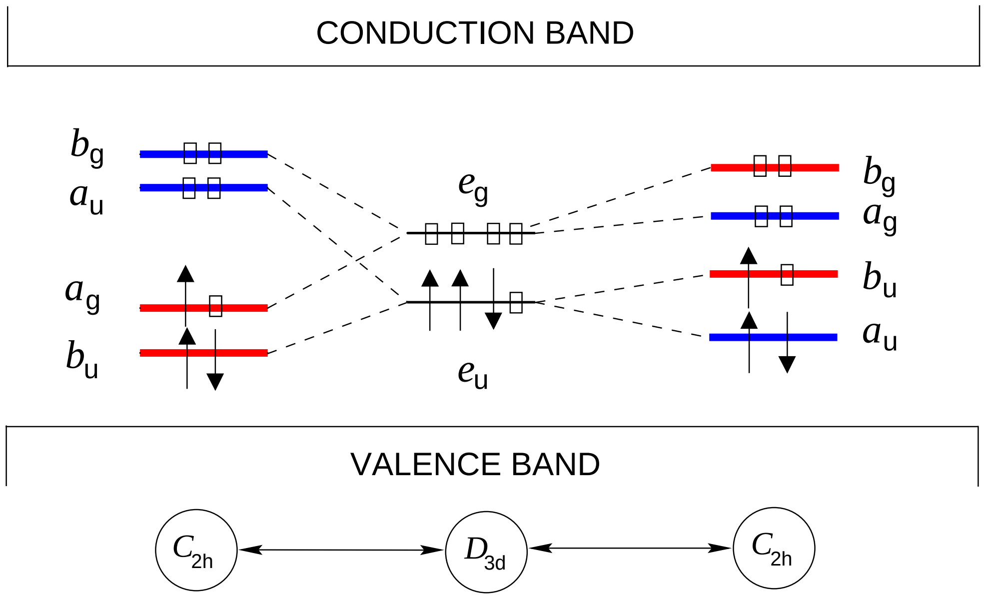

inwards distortion	undistorted	outwards distortion
"Rebonding-by-pairs Model	Breathing Model	"Resonant-bond" Model

Below: Projection of the wavefunction of the 2 highest occupied states onto the defect's mirror plane – inwards distortion.

b_u

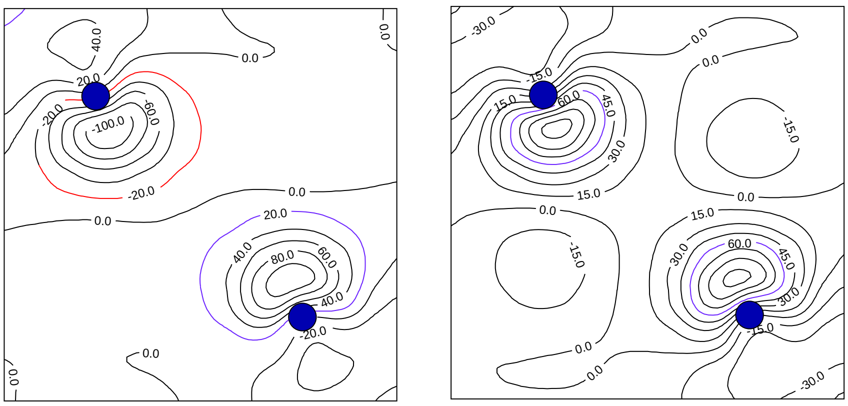

a_g

Results: D. Electrical levels

Table V. Calculated & observed electrical levels of V_2 in two different configurations: distorted (P) and undistorted (B). Values in eV.

Levels	C_{2h}	D_{3d}	Obs.
$(=/-)$	$E_c - 0.36^{(a)}$	$E_c - 0.33^{(a)}$	$E_c - 0.23$
	$E_c - 0.59^{(b)}$	$E_c - 0.56^{(b)}$	$E_c - 0.23$
$(-/0)$	$E_c - 0.63$	$E_c - 0.61$	$E_c - 0.43$
$(0/+)$	$E_v + 0.31$	$E_v + 0.46$	$E_v + 0.25$

The standard defect levels (markers) were the following:

- $(=/-)$: (a) Au–H_1 at $E_c - 0.19$ eV
  (b) Pt–H_2 at $E_c - 0.18$ eV
- $(-/0)$: interstitial-carbon (C_i) level at $E_c - 0.1$ eV
- $(0/+)$: C_i level at $E_v + 0.28$ eV

UNIVERSITY of EXETER